A transphyletic study of metazoan β-catenin protein complexes

Ivan Mbogo[1,5], Chihiro Kawano[1], Ryotaro Nakamura[1], Yuko Tsuchiya[2], Alejandro Villar-Briones[3,7], Yoshitoshi Hirao[3], Yuuri Yasuoka[4,8], Eisuke Hayakawa[1,6], Kentaro Tomii[2] and Hiroshi Watanabe[1]*

Abstract

Beta-catenin is essential for diverse biological processes, such as body axis determination and cell differentiation, during metazoan embryonic development. Beta-catenin is thought to exert such functions through complexes formed with various proteins. Although β-catenin complex proteins have been identified in several bilaterians, little is known about the structural and functional properties of β-catenin complexes in early metazoan evolution. In the present study, we performed a comparative analysis of β-catenin sequences in nonbilaterian lineages that diverged early in metazoan evolution. We also carried out transphyletic function experiments with β-catenin from nonbilaterian metazoans using developing *Xenopus* embryos, including secondary axis induction in embryos and proteomic analysis of β-catenin protein complexes. Comparative functional analysis of nonbilaterian β-catenins demonstrated sequence characteristics important for β-catenin functions, and the deep origin and evolutionary conservation of the cadherin–catenin complex. Proteins that co-immunoprecipitated with β-catenin included several proteins conserved among metazoans. These data provide new insights into the conserved repertoire of β-catenin complexes.

Keywords B-catenin, Metazoan, *Nematostella vectensis*, Protein complex

*Correspondence:
Hiroshi Watanabe
Hiroshi.watanabe@oist.jp
[1]Evolutionary Neurobiology Unit, Okinawa Institute of Science and Technology Graduate University, Okinawa, Japan
[2]Artificial Intelligence Research Center, National Institute of Advanced Industrial Science and Technology (AIST), Tokyo, Japan
[3]Instrumental Analysis Section, Okinawa Institute of Science and Technology Graduate University, Okinawa, Japan
[4]Marine Genomics Unit, Okinawa Institute of Science and Technology Graduate University, Okinawa, Japan
[5]Present address: Sysmex Corporation, Ltd. 1-5-1, Chuo-ku, Kobe 651-0073, Japan
[6]Present address: Department of Bioscience and Bioinformatics, Kyushu Institute of Technology, 680-4, Kawazu, Iizuka 820-8502, Fukuoka, Japan
[7]Present address: Project Planning and Implementation Section, Okinawa Institute of Science and Technology Graduate University, Okinawa, Japan
[8]Present address: Laboratory for Comprehensive Genomic Analysis, RIKEN Center for Integrative Medical Sciences, Yokohama, Japan

Background

Although the functions of β-catenin are diverse, its primary function in cell adhesion and Wnt signaling is well known. The structural role of β-catenin at the adherens junctions, in which the cytoplasmic domain of E-cadherin binds β-catenin which in turn binds α-catenin (Fig. 1), is crucial in promoting cell-to-cell adhesion [1–3]. Alpha-catenin binds to filamentous actin, linking the adherens junction complex to the cytoskeleton to maintain cell shape and strengthen cell-cell contacts. The signaling role of β-catenin is prominet within the canonical Wnt signaling pathway [4, 5]. In the absence of Wnt ligands, β-catenin that is not bound to E-cadherin is phosphorylated and subsequently degraded by the activity of a multiprotein destruction complex. The destruction complex is composed of Axin, APC, GSK3β, CK1α, and PP2A [6]. Canonical Wnt signaling is initiated when
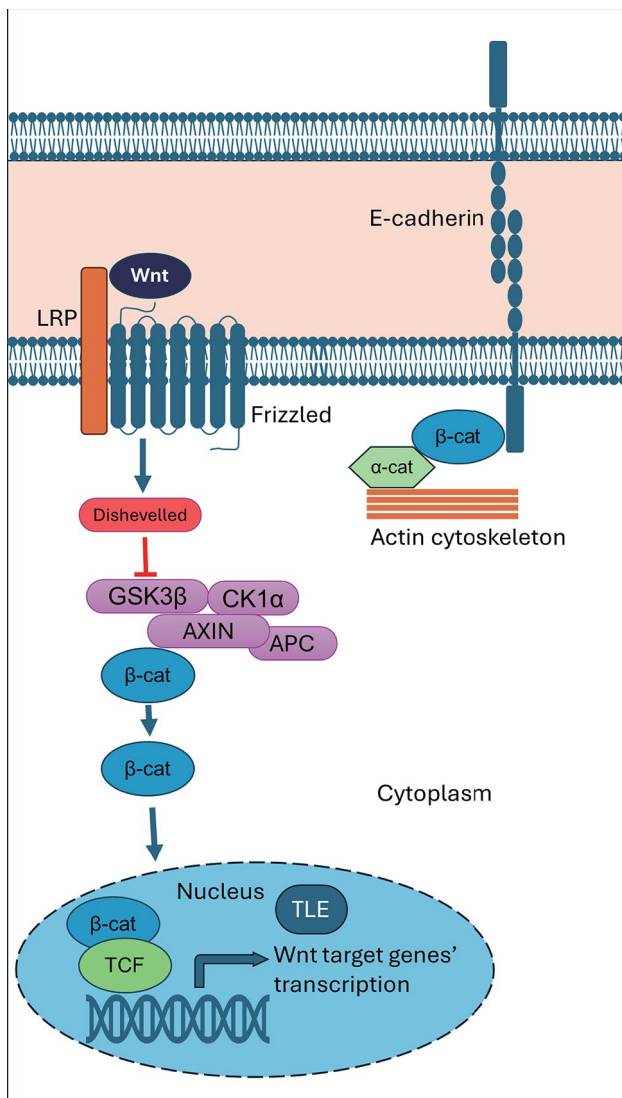
Fig. 1 Major functions of β-catenin in bilaterians. In signal transduction, in the presence of Wnt ligands, the β-catenin degradation complex is inhibited by Dishevelled. β-catenin accumulates in the cytoplasm and translocates to the nucleus, where it binds TCF and displaces the transcriptional repressor TLE, resulting in gene transcription of canonical Wnt signaling target genes. In structural roles, β-catenin contributes to E-cadherin-mediated cell-cell adhesion by linking E-cadherin to α-catenin, and reinforces cellular structure by binding α-catenin to the actin cytoskeleton

Wnt ligands bind to Frizzled and LRP5/6 receptors, inhibiting the destruction complex (Fig. 1), which results in the accumulation of β-catenin in the cytoplasm and its eventual translocation to the nucleus。In the nucleus, β-catenin functions as a co-transcription factor and cooperates with TCF/LEF transcription factors to activate expression of target genes involved in cell proliferation, differentiation, and survival.

Recent genome analysis of early-branching, nonbilaterian metazoans, including cnidarians, poriferans, and ctenophores, has revealed that many genes involved in

β-catenin signaling were acquired in parallel with the evolutionary emergence of the Metazoa. In Cnidaria, the closest sister lineage to Bilateria, the oral–aboral axis is the main body axis, and considerable evidence from research on selected cnidarians indicates that canonical Wnt signaling, which involves the β-catenin/TCF pathway, controls oral–aboral axis formation [7–11]. Indeed, in *Nematostella vectensis* (Anthozoa, Cnidaria), transplantation of a fragment from the blastopore lip, which has high β-catenin activity and will subsequently form the mouth, to the aboral ectoderm induces a secondary body axis [12]The ability of *Nematostella* Wnt1 to induce a secondary axis in *Xenopus* suggests the possible conservation of canonical Wnt function [6]. Similarly, transplantation of the hypostome to a different site causes a secondary body axis in *Hydra vulgaris* (Hydrozoa, Cnidaria) [13, 14]. These organizer functions of the blastopore/hypostome can be mimicked by enhancing β-catenin signals by treatment with a GSK3β inhibitor [13, 15]. In addition, β-catenin binds to and colocalizes with the cadherin–catenin cell adhesion complex in *Nematostella* [1, 2], as it does in bilaterians. In ctenophores and poriferans, the expression patterns of β-catenin signaling components are localized at specific positions along the developing embryo axis [4, 16–19]. In the ctenophore *Mnemiopsis leidyi*, in situ hybridizations revealed that *Wnt* and *β-catenin* genes are expressed post-gastrulation at the aboral and oral poles, respectively [4].

Data showing that multiple functions of β-catenin are already functional in early-branching metazoan lineages suggest that β-catenin's diverse protein complex repertoire was established, at least in part, early during metazoan evolution. One pioneering study in *Ephydatia muelleri* (Porifera), showed that cadherins and α-catenin bind to endogenous β-catenin, suggesting that the core complex of β-catenin machinery involved in cell–cell adhesion has deep evolutionary roots [3]. However, neither the complete picture of protein complexes formed by early β-catenin species nor commonalities in their components are known. To date, the β-catenin complex repertoire has been analyzed mainly in mammalian cell lines/tissues, including through studies employing immunoprecipitation with mass spectrometry (IP-MS) [19, 20]. Recently, in studies of β-catenin protein–protein interactions (PPIs), researchers have begun to move from cell to tissue culture systems, allowing identification of tissue-specific PPIs [21, 22].

To compare proteins that bind to β-catenin in various early-branching metazoans, we employed a transphyletic experimental approach, in which we examined proteins of the complex formed by heterologous β-catenins expressed in developing *Xenopus* embryos. The transphyletic approach is classical, but remains an effective

technique for testing evolutionary conservation of protein functions and gene-regulatory networks, especially in comparative analyses of diverse phyla, including nonmodel early-branching nonbilaterians [23–28]. This system also allows an experimental comparison among β-catenins from phylogenetically distant species for β-catenin complexes associated with specific biological contexts.

In the present study, to gain insights into the evolution of the β-catenin protein complex, we performed a comparative analysis of β-catenin sequences from nonbilaterian lineages that diverged early in metazoan evolution. Examining these nonbilaterian β-catenins, we focused particularly on amino acid residues and motifs known to play roles in β-catenin function in bilaterians. We next performed a transphyletic experiment with β-catenin derived from a nonbilaterian metazoan using developing *Xenopus* embryos, one of the best experimental systems for verifying organizer-inducing activity of β-catenin. Finally, we carried out a proteomic survey of proteins immunoprecipitated with nonbilaterian β-catenin from *Xenopus* gastrula embryos to develop a candidate list of evolutionarily conserved protein components of the β-catenin machinery.

Results

Sequence comparisons and 3D structures of metazoan β-catenins

In our analysis of the early evolution of the β-catenin complex, we first examined conservation of β-catenin sequences of early-branching nonbilaterians (Fig. 2). This is important for understanding post-translational modifications and direct protein interaction sites. As a reference structure, we included ARM6, a β-catenin-like protein from the choanoflagellate, *Salpingoeca rosetta*. Choanoflagellates are a sister group of Metazoa. Choanoflagellate ARM6 is ancestral to metazoan β-catenin and Adenomatous Polyposis Coli (APC) groups with fewer armadillo repeats (Fig. 2A, B) [29]. Overall, cnidarian and poriferan β-catenins share many functional motifs with bilaterian β-catenin, but in ctenophores differences are observed particularly in the C-terminal region, in which motifs A and B are absent. In ARM6 of Choanoflagellate, except for a few phosphorylation sites, most functional motifs are not conserved.

Our comparative analyses suggest that GSK3β and CK1α phosphorylation sites critical for β-catenin degradation are conserved in all metazoans, except for *Hydra*, which lacks the site corresponding to S37 (Fig. 2B, S1, S2). Interestingly, in unicellular *S. rosetta*, two residues corresponding to S33 & T41 were also conserved. The central domain is the primary interaction site for several proteins, including TCF and Cadherin1 (CDH1) [30, 31]. A high degree of conservation was observed in Bilateria,

Cnidaria, and Porifera in the central region (Fig. 2B). Cnidarian and poriferan β-catenins displayed full conservation of the three critical lysine residues (K312, K335, and K435 in mouse β-catenin) and others (Y331, D390, and R582) that are required for E-cadherin binding [30, 31]. Among these sites, only two lysines, K312 and K435, were conserved in Ctenophora (Fig. 2B, S1).

Three arginine residues of mouse β-catenin, R474, R582, and R612, are important in binding to TCF [30, 32]. These amino acids are conserved in Cnidaria and Porifera. However, in Ctenophora, R582 and R612 are not conserved and the residue corresponding to R474 is substituted with a lysine residue. To gain further insight into the influence of these differences on binding of TCF, we investigated other amino acids—K312, N426, K435, R469, H470, K508, H578, and Y654—thought to be involved in β-catenin–TCF interactions in mice [30–33]] (Fig. 2B, S1). Similar to the three important arginine residues (R474/R582/R612) mentioned above, these amino acids are also common to Bilateria, Cnidaria, and Porifera, and all except H578 and Y654 are conserved in Ctenophora. Interestingly, most of these amino acids that function in binding of β-catenin to TCF are not conserved in *S. rosetta*. However, *S. rosetta* ARM6 has an asparagine corresponding to N426 and an arginine, which has chemical properties similar to those of lysine, at a position corresponding to lysine (K312).

The C-terminus of β-catenin, which has a transactivation domain, is important for regulation of gene expression by the β-catenin/TCF complex [34, 35]. Its signaling ability is probably attributable to two motifs, A and B [35–38]. Alignment combined with Multiple Expectation maximization for Motif Elicitation (MEME) analysis confirmed that motif A is present only in Bilateria and Cnidaria, whereas motif B is also present in Porifera (Fig. 2B, S1, S3). In contrast, neither motif A or B is found in ctenophore β-catenin and choanoflagellate ARM6.

Finally, we compared amino acids required for binding to α-catenin. The α-catenin binding site in β-catenin was previously narrowed down to amino acids 118–146 (in mice) [39]. Metazoan-wide conservation across this region is not very high, except for a few residues. In mouse β-catenin, Y142 is vital for α-catenin binding, since mutation to alanine eliminates interaction between β-catenin and α-catenin [39]. The site corresponding to Y142 is conserved in all metazoans (Fig. 2B, S1, S4). Two acidic residues, D144 and E147, also affect interaction with α-catenin [40]. D144 is not conserved among poriferans. *Salpingoecca rosetta* exhibits a large insertion sequence in this region, which precluded accurate verification.

Beta-catenin sequences from *Xenopus laevis* (Vertebrata), *Nematostella vectensis* (Cnidaria), *Ephydatia fluviatilis* (Porifera), *Bolinopsis mikado* (Ctenophora), and
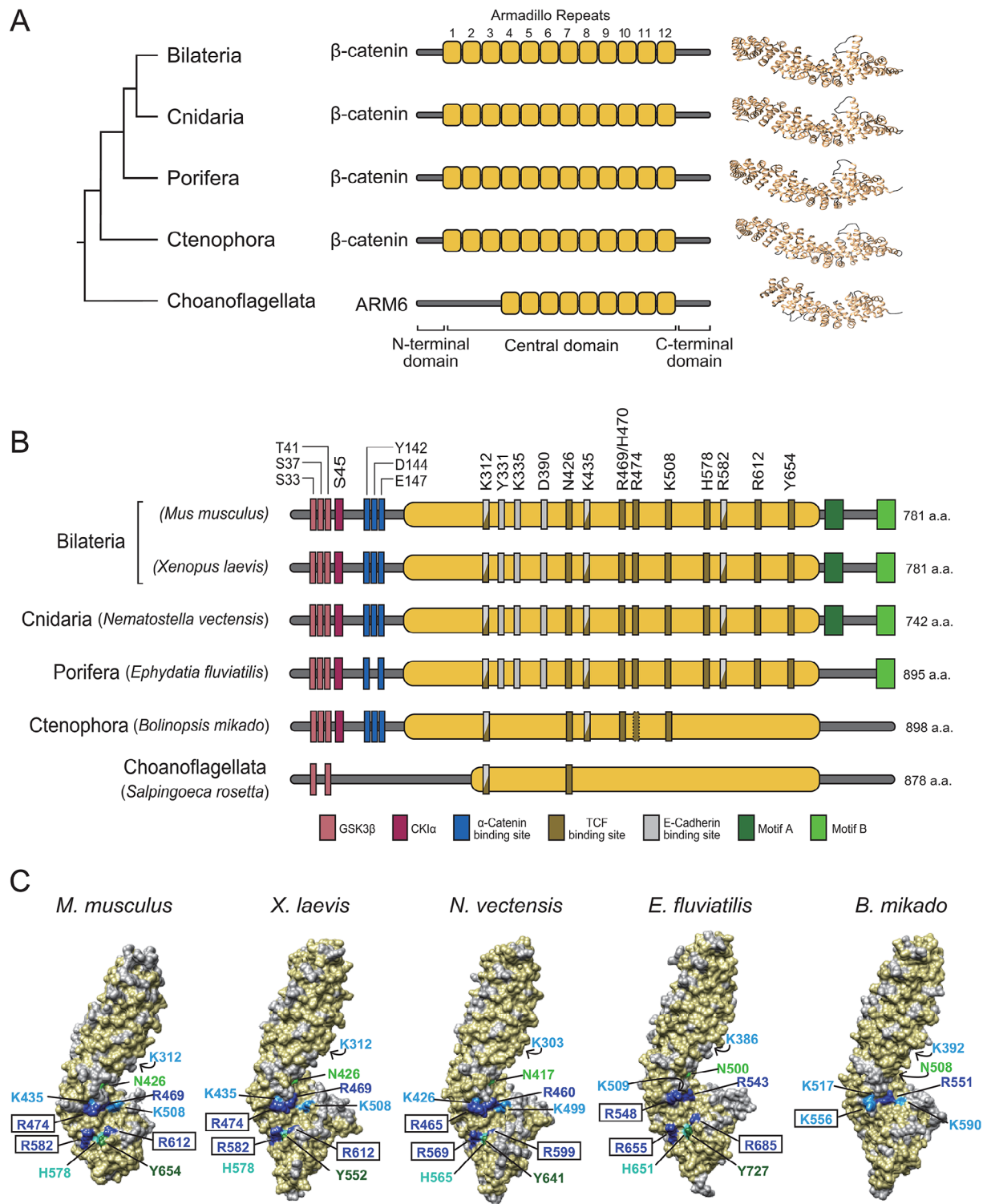
Fig. 2 Primary and 3D structures of nonbilaterian β-catenins. (**A**) Overview of phylogeny and structure of β-catenins of early-branching (nonbilaterian) metazoans and ARM6 protein of the unicellular sister taxon, Choanoflagellata. (**B**) Domain organizations of β-catenin proteins. Metazoan β-catenins show a high degree of conservation of the central region, GSK3β/CK1α phosphorylation sites, and αE-catenin binding sites. At the C-terminus, motif A is conserved in only Bilateria and Cnidaria, whereas motif B is shared among all metazoan lineages, except for Ctenophora. In the choanoflagellate, *Salpingoeca rosetta*, possible GSK3β phosphorylation sites (S33/T41) were identified. (B) Surface depictions of β-catenin homology structural models were compared with mouse β-catenin. This confirmed that the three crucial arginine residues (dark blue) of nonbilaterians were localized similarly to mouse and *Xenopus* β-catenins. K556, R551, and K590 of *B. mikado* β-catenin were located at positions corresponding to mouse β-catenin R474, R469, and K508, but the R582, H578, R612, and Y654 assembly of mouse β-catenin is completely absent in *B. mikado* β-catenin. Structures visualized using UCSF Chimera software

ARM6 of *S. rosetta* were next used in homology modeling against the crystal structure of mouse β-catenin (PDB ID: 4ev8) to investigate structural evolution. Phi-Psi distribution of Ramachandran plots generated with PROCHECK indicated that over 90% of amino acids in modeled structures were in favored positions (Fig. S5). Despite amino acid variations of β-catenin observed among metazoans (Fig. S6), the structure of the predicted armadillo repeat region of β-catenin appears to have remained stable since the emergence of the Metazoa. Interestingly, between residues 452 and 878, the *S. rosetta* ARM6 protein possesses a structure that resembles metazoan β-catenins (Fig. S7). However, *S. rosetta* ARM6 has a short loop, whereas metazoan β-catenins have a long loop between armadillo repeats 10 and 11, indicating that this is likely a metazoan invention (Fig. 2A). The armadillo repeat region contains multiple amino acids that either are or may be involved in binding TCF (Fig. 2B). These amino acids are conserved in β-catenins in bilaterians, cnidarians and poriferans. We also demonstrated spatial conservation of these amino acids. Thus, in addition to sequence similarities, orientations of TCF-binding amino acids are highly conserved in β-catenin from Bilateria, Cnidaria, and Porifera (Fig. 2C). In Ctenophora, homology was observed only in a few amino acids.

Given their structural similarities, the next question is: To what extent are the functions of β-catenins conserved?

Functional analysis of nonbilaterian β-catenins, using mainly *Nematostella*, shows that β-catenin is important in the blastopore organizer and during gastrulation and subsequent endoderm fate determination, although the timing and embryonic region in which β-catenin is active in the nucleus remain controversial [7, 11, 41, 42]. On the other hand, in poriferans and ctenophores, knowledge of β-catenin function is much more limited [3, 4, 18, 43]. During development of *Mnemiopsis leidyi* (Ctenophora), perturbation of classical β-catenin signaling had limited effect [4]. Classical β-catenin complexes have also been reported in adult *Ephydatia*, but their functions remain unknown [3].

Comparison of axis-inducing activity of metazoan β-catenins in *Xenopus* embryos

To investigate the conservation of β-catenin activity, we performed a secondary axis induction assay using an ectopic expression system with *Xenopus* embryos. In vivo embryonic systems, which require a variety of cellular developmental events, such as epithelial formation, active cell division, and formation of signal centers necessary for body axis patterning, are ideal for comprehensive functional surveys of the β-catenin complex. Differences in codons in mRNAs of different organisms can affect rates of translation when expressed in other organisms.

We began our analyses of functional conservation by optimizing the amount of mRNA injected to achieve expression of relatively similar levels of FLAG-tagged proteins (Fig. S8A). For all metazoan β-catenins, FLAG-tagged β-catenin protein was observed at the expected band sizes. However, we did not observe expression of *S. rosetta* ARM6 in *Xenopus*, even when the amount of injected mRNA was increased (Fig. S8B). Therefore, the following analysis was performed using only metazoan β-catenins.

To test whether basal metazoan β-catenins are functional, we injected them into the ventral equatorial region of a single blastomere in *Xenopus* 4-cell embryos. Figure 3B shows that injection of 100 pg mRNA resulted in expression of FLAG-tagged β-catenin proteins. These results showed that *N. vectensis* and *E. fluviatilis* β-catenin induced a secondary body axis similar to that induced by *X. laevis* β-catenin (Fig. 3A, C). In contrast, *B. mikado* β-catenin did not induce a secondary axis. Even when *B. mikado* β-catenin mRNA was injected at high concentrations (500 pg), only protrusion-like structures without head characteristics appeared in some embryos (Fig. S9). This suggests that the lack of secondary axis-inducing ability of *B. mikado* β-catenin is due to differences in signals it can activate, rather than to weakness of activation.

To further determine whether basal metazoan β-catenins can drive β-catenin/TCF signaling, a TOPflash luciferase assay using *Xenopus* embryos was performed [44, 45]. Consistent with secondary axis induction experiments, there was a significant increase in luciferase activity following expression of *X. laevis*, *N. vectensis*, and *E. fluviatilis* β-catenin (Fig. 3D), confirming that signaling activity of β-catenin is conserved in Cnidaria and Porifera. In contrast, expression of *B. mikado* β-catenin did not increase luciferase activity. This suggests reduced conservation of amino acids necessary for TCF binding in ctenophore β-catenins (Fig. 2B). Additionally, together with the finding that β-catenin activation in *Mnemiopsis* does not clearly affect conserved functions, such as body axis formation [4], these data suggest that ctenophore β-catenin does not contribute significantly to canonical Wnt signaling (Wnt/β-catenin/TCF signaling). The capacity of cnidarian and poriferan β-catenins to induce phenotypes similar to that of *Xenopus* β-catenin suggests that they all form a common protein complex in *Xenopus* embryos. To test this hypothesis, we next examined the protein complex formed by each β-catenin in developing *Xenopus* embryos.

Proteomic analysis of β-catenin protein complexes

To investigate protein complexes made by each basal metazoan β-catenin in developing *Xenopus* embryos, FLAG-tagged β-catenin was immunoprecipitated from
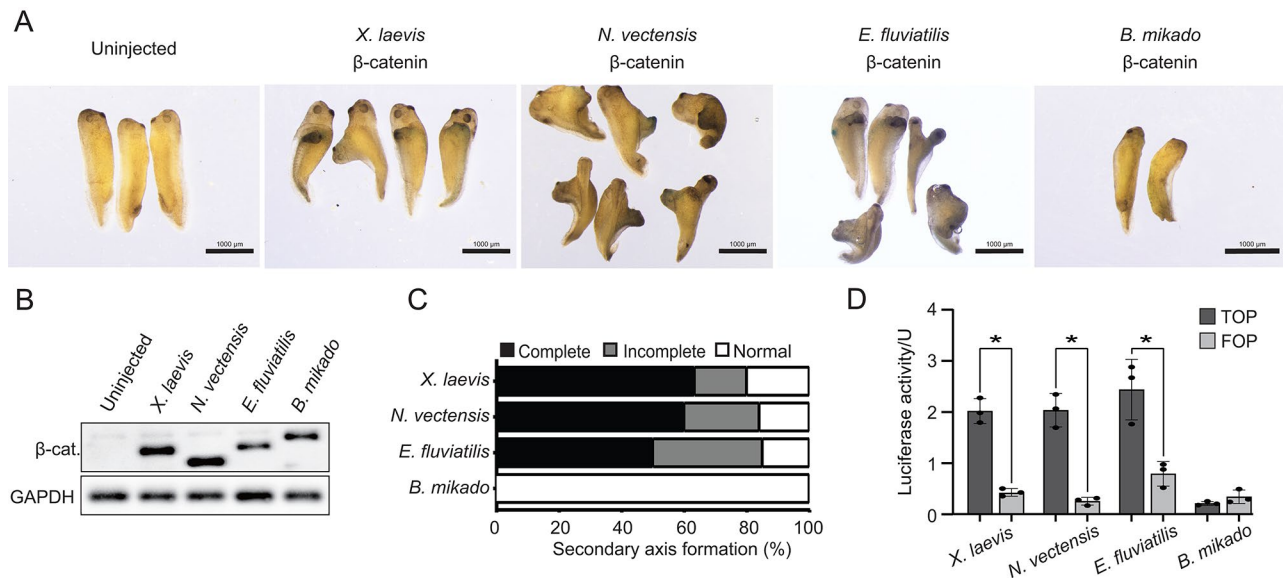
Fig. 3 *Xenopus* secondary axis induction by nonbilaterian β-catenins. (**A**) Cnidarian (*N. vectensis*) and poriferan (*E. fluviatilis*) β-catenins (100 pg mRNA) induced a secondary body axis similar to that induced by *Xenopus* β-catenin. Ctenophore (*B. mikado*) β-catenin showed no inductive activity. (**B**) Western blot analysis of Flag-tagged β-catenins confirmed the expression of nonbilaterian β-catenin proteins in *Xenopus* embryos. (**C**) The majority of secondary body axes induced by injection of *X. laevis* (*n* = 24), *N. vectensis* (*n* = 20), and *E. fluviatilis* (*n* = 18) β-catenin mRNAs (100 pg) were complete (the second axis had a pair of eyes and a cement gland). This was followed by incomplete axis inductions in which head features were not fully developed. Secondary axes were not observed in embryos injected with *B. mikado* β-catenin mRNA (100 pg) (*n* = 19). (D) Expression of *X. laevis*, *N. vectensis*, and *E. fluviatilis* FLAG-tagged β-catenin mRNA (100 pg) in *Xenopus* embryos resulted in a significant increase in β-catenin TOPflash activity. No detectable level of TOPflash activation was observed by expression of *B. mikado* β-catenin. Asterisks denote statistical significance $P < 0.0001$ (Two-way ANOVA). This result was reproduced in two independent experiments

homogenates at gastrula stage 11, and proteomic analysis of resulting protein complexes was performed. Western blotting confirmed that comparable amounts of exogenous FLAG-tagged β-catenin proteins were immunoprecipitated (Fig. S10). Subsequently, interacting proteins were identified using liquid chromatography with tandem mass spectrometry. An IgG control analysis from uninjected embryos was also included. To reduce false positives in identified proteins, only proteins with an abundance ratio greater than or equal to 2 (*P*-value < 0.05) are generally used as a threshold for "true" interactions. The presence of known bilaterian β-catenin interacting proteins confirmed that identified proteins represented "true" interactions (Fig. 4A, Table S1). Figure 4B shows a schematic of proteins co-immunoprecipitated with each β-catenin species. A number of proteins, including Cadherin (CDH), have been identified as interacting partners with all exogenous metazoan β-catenins. Our BLAST search confirmed that many of them have protein homologs in nonbilaterian metazoans.

Unexpectedly, many metabolism-related proteins, such as DHRS12, PHGDH, SDR39U1, and MOCS3, were commonly detected in bilaterian/nonbilaterian β-catenin complexes (Fig. 5). Although we found no reports that these enzymes interact with β-catenin, and their physiological significance in the β-catenin complex is currently unknown, it has been shown that overexpression of DHRS12 inhibits β-catenin signaling in human cell lines [46]. Another group of highly conserved components of the β-catenin complex includes proteins associated with cell adhesion. Since conservation of CDH1 binding sites on β-catenin is very high among metazoans (Fig. 2B, Fig. S1), it is unsurprising that CDH1 was precipitated by all β-catenins.

Interestingly, *E. fluviatilis* β-catenin was unable to immunoprecipitate *X. laevis* α-catenin at detectable levels. This was also confirmed in western blotting analysis (Fig. S11). Poriferan β-catenins do not have the conserved amino acids required for binding to α-catenin (Fig. S4). On the other hand, binding of endogenous β-catenin and α-catenin has been observed in the poriferan, *Ephydatia muelleri* [3]. This suggests that poriferan ancestors evolved a unique interaction of β- and α-catenin. Given that β-catenin proteins in a broad array of nonbilaterians bind α-catenin and phylogenetically distant CDH1 proteins, this finding suggests that β-catenin complex functions involved in the adherens junction were acquired among the earliest metazoans and remain highly conserved, although there were unique modifications in the Porifera.

Since organizer-inducing activity was observed in bilaterian, cnidarian, and poriferan β-catenins in developing *Xenopus* embryos, we expected to detect protein complexes specific to these β-catenin immunoprecipitates.
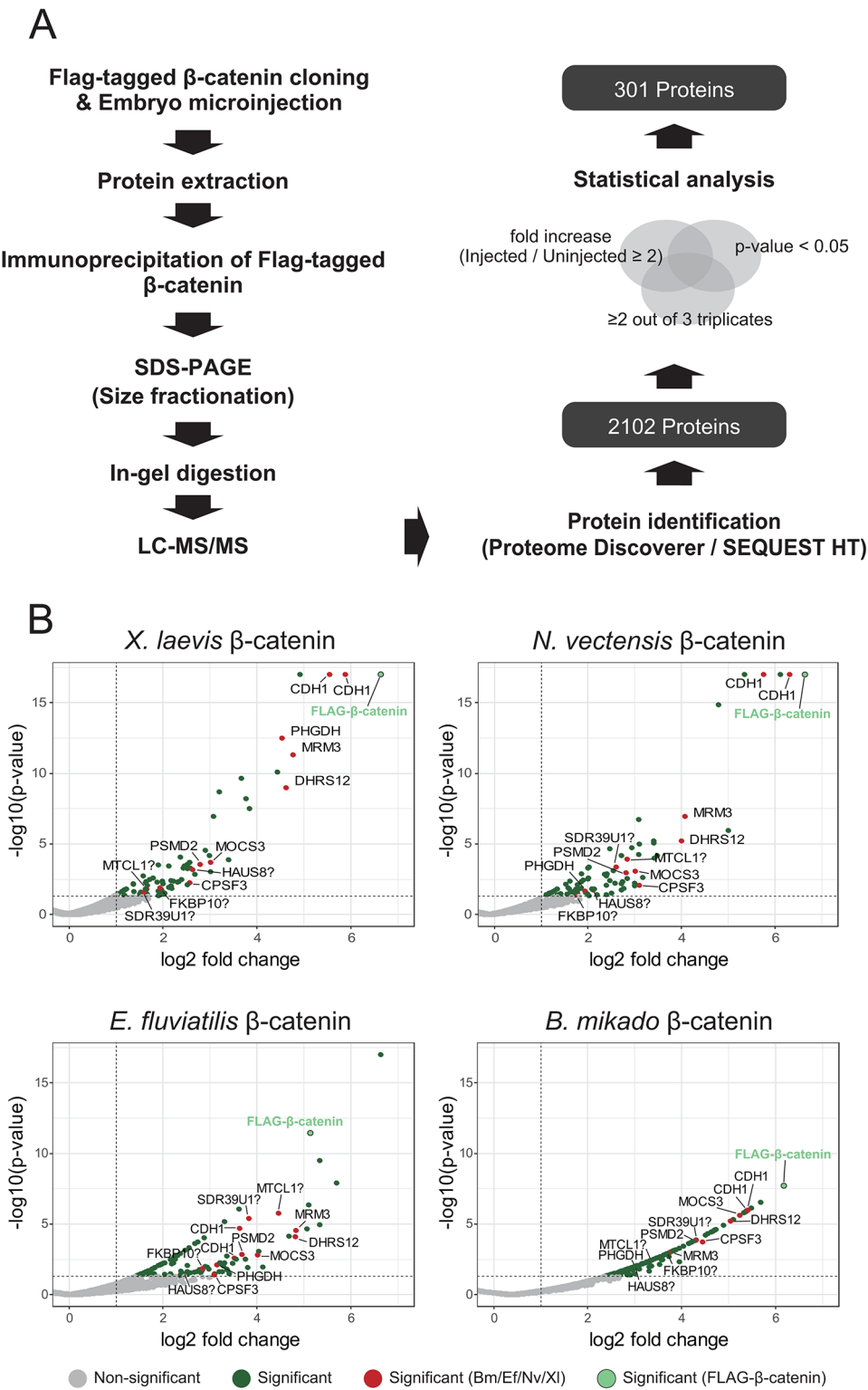
Fig. 4 Precipitation of β-catenin interacting proteins. (**A**) Scheme of our IP-MS analysis of β-catenin protein complexes. (**B**) Mass spectrometry volcano plots resulting from analysis of enriched metazoan FLAG-tagged β-catenins expressed in *Xenopus* embryos. High confidence proteins (1% FDR), with a fold abundance ratio ≥ 2 and *P* < 0.05, were considered "true" interactions
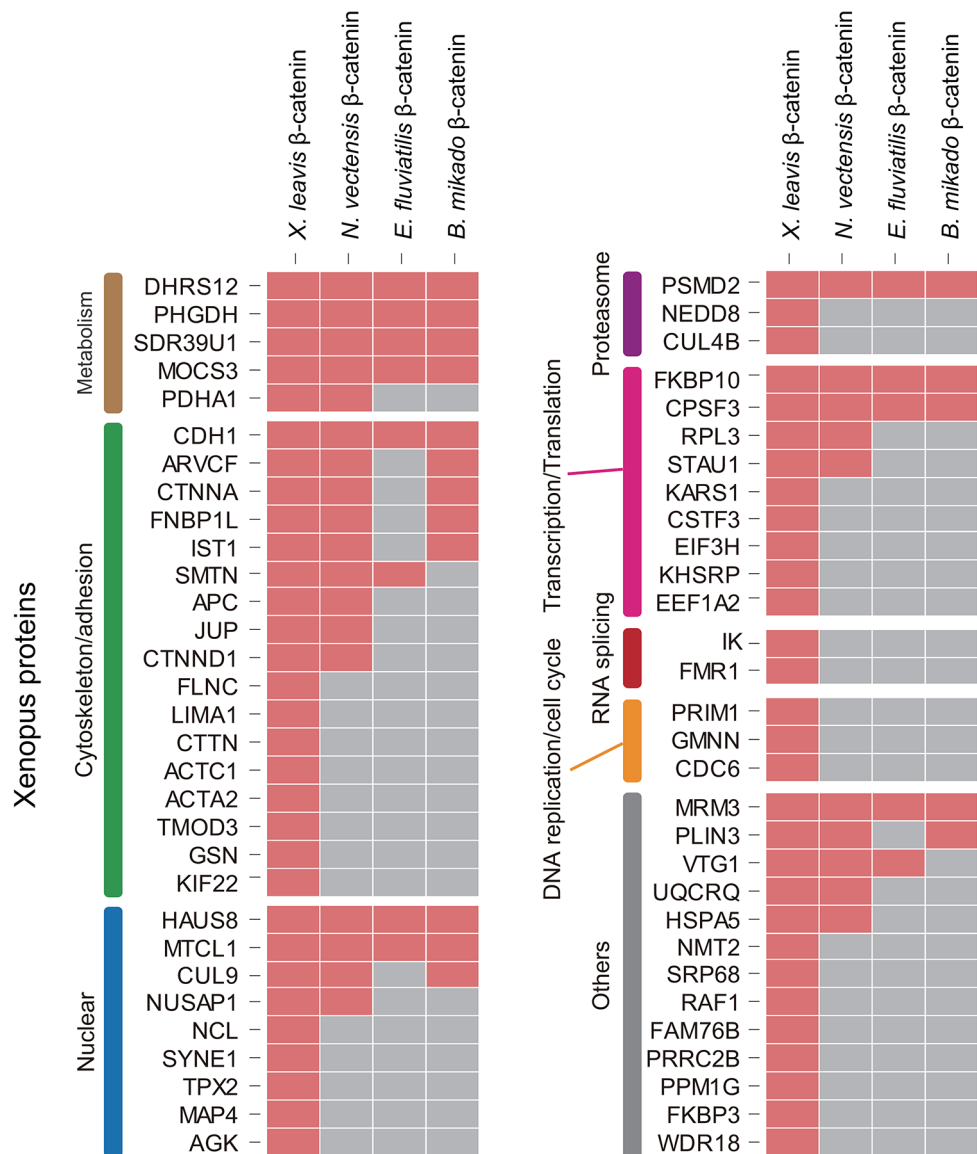
Fig. 5 Potential evolutionarily conserved β-catenin interactions. Several proteins, e.g., CDH1, ARVCF, CTNNA1, that interact with β-catenin mainly in bilaterian models, formed complexes with basal metazoan β-catenins. Furthermore, new interactions were identified that may shed additional light on functional evolution of β-catenin protein machinery in metazoans

However, proteomic analysis detected only a few proteins common to bilaterian/cnidarian/poriferan β-catenins. Smoothelin (SMTN) was identified as a binding protein common to β-catenin of *X. laevis*, *N. vectensis*, and *E. fluviatilis*. In bilaterians, SMTN binds Cortactin (CTTN) and stabilizes the cortical actin meshwork of epithelial cell membrane [47]. Cortactin binds β-catenin, α-catenin, and p120 catenin (catenin delta-1/ CTNND1) and is important for the function of adherens junctions [48]. VTG1, which has an unknown function, was also detected in this group; however, even though gene homologs of SMTN and VTG1 exist in *X. laevis* and *N. vectensis*, they are not in the transcriptome of *E. fluviatilis* [49] (Fig. S12).

Discussion

Several studies have suggested that β-catenin was involved in the rise of multicellularity and further evolution of complex body organization. However, little is known about structural attributes of β-catenin that underlie its various functions, and the evolutionary process of β-catenin machinery. In the present study,, we performed a detailed sequence analysis of metazoan β-catenins and utilized structural, proteomic, and functional analyses to understand evolutionary dynamics of the β-catenin complex.

Conserved and lineage-specific features of β-catenin cell adhesion complexes

Key lysine residues (K312 and K435) for binding E-cadherin are conserved in all metazoan β-catenins, and in fact, it was confirmed that E-cadherin co-immunoprecipitates with all metazoan β-catenins from *Xenopus* embryos. It has been suggested that Y331, K335, D390, and R582 residues of mouse β-catenin are important for binding to an intercellular domain of E-cadherin [31]. However, these residues are conserved in Cnidaria and Porifera, but not in Ctenophora. Considering that *Xenopus* E-cadherin binds with all metazoan β-catenins, including those from Ctenophora, these amino acids appear non-essential for binding to E-cadherin. The inability of poriferan β-catenin to bind *Xenopus* α-catenin was surprising, as previous research had confirmed endogenous interaction of these proteins in *Ephydatia* [3]. The cause appears to be the charge distribution near the critical tyrosine residue in the α-catenin binding site. In mouse β-catenin, the hydroxyl group of Y142 is proximal to two acidic amino acids, D144 and E147. Mutating these residues or introducing a negative charge on Y142 could alter charge distribution, preventing α-catenin binding [40]. In both *Ephydatia muelleri* and *Ephydatia fluviatilis*, acidic residues are conserved at the site corresponding to E147, whereas D144 is substituted for the neutral glycine, possibly impeding or weakening α-catenin binding. This implies that poriferan β-catenin and α-catenin co-evolved in ways that either enable or strengthen interaction. Details of molecular features of the cell adhesion system of poriferan epithelia have not yet been clarified. Furthermore, in Ctenophora, genetic peculiarities of elements involved in cell adhesion machinery have been reported [31]. Understanding the functions of cadherins and α-catenins in Ctenophora and Porifera remains for further study.

Organizer induction and β-catenin signaling

The key to explaining the organizer induction results might have been co-immunoprecipitation of TCF with β-catenin, but our IP-MS did not identify any TCF peptides. This is probably because the β-catenin/TCF complex is not very stable. Indeed, previous β-catenin IP-MS studies have also been unsuccessful at detecting β-catenin-TCF interaction [20, 22, 50]. Further experimental optimization is needed to discover the molecular organization of the transcription regulatory machinery formed by β-catenin and transcription factors such as TCF, but comparisons of the function and sequence of β-catenin in basal metazoans still provided new insights. Some amino acids of β-catenin that are key to binding TCF are conserved in all metazoans, but four sites corresponding to R582, H578, R612, and Y654 in mouse β-catenin are not conserved in ctenophores. However,

a previous study using *X. laevis* β-catenin showed that mutations R612A and Y654A do not significantly affect TCF interaction [33]. These may, therefore, not be evolutionarily critical in binding TCF. We also observed domain differences in the C-termini of ctenophore β-catenins. Previous studies have shown that β-catenin C-termini can function as transcriptional activators when fused to TCF [51, 52]. Furthermore, a β-catenin C-terminus-LEF1 fusion is sufficient for secondary body axis induction in *Xenopus* [34]. Two motifs, A and B, have previously been identified in the C-terminus [36]. Motif A was confined to bilaterians and cnidarians. It is localized in the Helix-C region, a key region for β-catenin transcription activity [53]. However, motif A is probably not essential for organizer induction, as it is absent in *E. fluviatilis* β-catenin that still managed to drive secondary axis induction. Our focus then turned to motif B, which is present in all metazoans except ctenophores. A recent study showed that mutation of this domain resulted in decreased TCF-dependent transcriptional activity [37]. Therefore, organizer induction capacity may depend on the interaction at R582/H578 and motif B with transcription factors such as TCF. The inability of *B. mikado* β-catenin to induce a secondary body axis could be because it cannot activate downstream target genes of β-catenin/TCF (Fig. 3D), possibly due to insufficient interaction at motif B with endogenous proteins.

β-catenin and microtubule functions

Our study uncovered several centrosome-related proteins. Centrosomal localization of β-catenin has been observed in *Caenorhabditis elegans* (Nematoda) and *Platynereis dumerilii* (Annelida) [54–57]. However, although it has been suggested that centrosomal accumulation is conserved, there is no evidence for this in nonbilaterians. HAUS8, now identified as a member of the β-catenin complex, is part of a multi-subunit protein complex that controls centrosome and spindle integrity [58]. Depletion of HAUS8 resulted in centrosome defects, delayed mitosis, and increased aneuploidy [59]. Since β-catenin localization at centrosomes is associated with mitotic progression [60], it is plausible that HAUS8 and β-catenin interact to promote mitosis. The HAUS8 gene is absent before the Bilateria and Cnidaria, and it may represent a new interaction adopted by these common ancestors to control cell division. Several other β-catenin partners are common to Bilateria and Cnidaria, including a group of proteins essential for microtubule formation. One of these, APC, forms a complex with β-catenin in bilaterians [61, 62]. As expected, we found that *Xenopus* APC binds to the complex of *X. laevis* and *N. vectensis* β-catenin proteins. APC was previously detected at centrosomes in interphase and mitosis [63, 64]. Recent expression studies showed that APC

functions at centrosomes by stimulating microtubule growth, since expression of a truncated APC reduced the rate of microtubule growth [65]. Finally, a microtubule-associated protein, NuSAP1, was identified as interacting with both *X. laevis* and *N. vectensis* β-catenin. NuSAP1 activates β-catenin signaling and its depletion results in abnormal mitotic spindles, followed by abnormal chromosome segregation and cytokinesis [66]. These proteins may have been critical in strengthening β-catenin functionality in the last common ancestor of the Bilateria and Cnidaria.

Conclusions

In this study, we conducted a comprehensive analysis of sequences, structures, and binding protein repertoires of β-catenins, a metazoan invention that is responsible for the oldest multifunctional signal pathway. We particularly focused on comparisons using primary and 3D structure predictions, and transphyletic functional analysis, using developing *Xenopus* embryos, a biological context in which β-catenin serves an important function. Our results show high conservation of β-catenin sequences in Bilateria/Cnidaria/Porifera, and clarify the uniqueness of β-catenin in Ctenophora, the earliest branching metazoan lineage. Although proteomic analysis did not identify proteins associated with the functional gap between Bilateria/Cnidaria/Porifera and Ctenophora β-catenin complexes, structural and functional comparisons revealed the most evolutionarily conserved β-catenin region essential for interacting with TCF. Comparable proteomic analysis of various metazoan β-catenin complexes identified many complex constituent proteins, including novel members, and revealed their repertoires and phylogenetic distribution. These phylum-wide β-catenin complex lists provide foundational insights for future analysis to follow the evolutionary process of β-catenin function.

Materials and methods

Structural evolution of β-catenin

Bidirectional protein BLAST searches using mouse β-catenin were carried out against various databases to extract metazoan β-catenin sequences from representative bilaterians (*Xenopus laevis*; NP_001080749.1), Cnidaria (*Nematostella vectensis*: XP_001647517.2) and, as an outgroup, *Choanoflagellata* (*Salpingoecca rosetta*: XP_004991097.1). Potential β-catenin transcripts for *Bolinopsis mikado* (c56689_g1_i1) and *Ephydatia fluviatilis* (m.31095) were identified by BLAST analysis on their transcriptomes. These were then translated using the ExPASy Translate Tool. Amino acid sequences of *E. fluviatilis* and *B. mikado* were aligned using MIQS, a scoring matrix optimized to detect distant homologs [67]. The putative β-catenin of *Salpingoeca* was aligned with

structurally known β-catenin using HHpred [68]. Due to a high substitution rate at the N- and C-termini, alignment was focused on the region from the α-catenin binding site to the 12th armadillo repeat. Multiple sequence alignments of β-catenin were calculated using FAMSA [69]. β-catenin 3D models were built using MODELLER v9.20 [70], based on alignments of targeted, structurally known β-catenins, calculated using FORTE/ DELTA-FORTE, which are profile–profile alignment methods [71]. Structural models predicted with PROCHECK [72] which generates Ramachandran plots, showed the distribution of combinations of backbone dihedral angles Phi and Psi [73]. Visualization of final model structures was carried out using UCSF Chimera (Version 1.15) [74].

For domain analysis, all sequences were aligned using MUSCLE [75]. Manual curation was then undertaken to match the current alignment with the alignment used for structural analysis, resulting in a final high-quality alignment. To identify possible motifs at the C-terminus, MEME analysis was performed on unaligned sequences using MEME Suite 5.3.4 [76] with a maximum motif width of 20.

Animal culture

Adult male and female *Xenopus laevis* were purchased from *Xenopus* Aquaculture for Teaching Materials (Ibaraki Prefecture, Japan) and maintained in our frog facility. All experiments with *X. laevis* were approved by the Animal Care and Use Committees at Okinawa Institute of Science and Technology Graduate University.

Gene cloning and mRNA preparation

Total RNA was extracted from planula stage *N. vectensis*, larval stage *B. mikado*, and juvenile *E. fluviatilis* using RNeasy Mini Kit (Qiagen) following manufacturer's guidelines. cDNA synthesis was carried out from 1 μg of total RNA using SuperScript IV First-Strand Synthesis System (Thermo Fisher Scientific). PCR based cloning using Q5 High-Fidelity DNA Polymerase (NEB) with specified (Table S3). Restriction digestion sites were inserted in both forward and reverse primers to allow insertion into pCS2+plasmids. Furthermore, a Kozak sequence and FLAG-tag coding sequence were inserted into the forward primer. PCR reactions were carried out using a Mastercycler Nexus GX2 (Eppendorf) in 50 μl reactions. The cloned genes were then sequenced using cloning and internal primers to confirm their cDNA sequences. Following plasmid linearization, 1 μg of linearized DNA was used for mRNA synthesis with an mMESSAGE mMACHINE SP6 Transcription Kit (Ambion) following the manufacturer's guidelines, with a few changes. Briefly, components of the transcription kit were thawed at room temperature and then kept on ice apart from the 10x Reaction buffer. Next, the reaction

mix was set up by combining 10 μL 2X NTP/CAP, 2 μL 10x Reaction buffer, 1 μg linear template DNA, 2 μL enzyme mix, and an appropriate amount of nuclease-free water to a final volume of 20 μL. The reaction was mixed by pipetting and incubated for 4 h at 37 °C. 1 μL TURBO DNase was then added to the reaction mix and incubated at 37 °C for 20 min. Finally, a MEGAclear Transcription Clean-Up Kit (Ambion) was used to purify synthesized mRNA following the manufacturer's instructions. The mRNA concentration was measured using a Nanodrop 2000c spectrophotometer (Thermo Fisher Scientific), and RNA quality was confirmed using an Agilent 4200 Tapestation (Agilent). The mRNA was then aliquoted and stored at −80 °C.

Secondary axis induction assay

Xenopus laevis embryos were obtained by in vitro fertilization [77] and staged according to Nieuwkoop and Faber [78]. mRNA (100 pg) was co-injected with tracer LacZ mRNA (encoding β-galactosidase) (25 pg) into the ventral equatorial region of one blastomere at the 4-cell stage. Injected embryos were then incubated overnight at 20 °C in 1× Steinberg solution containing 5% Ficoll and then transferred into 0.1× Steinberg until stage 37, followed by X-gal staining. Axis duplication success was scored as "Complete" if the second axis had eyes and a cement gland, "Incomplete" if head features of the secondary axis were not fully developed, and "Normal" if there was only one axis. For each experiment, uninjected and LacZ mRNA-injected embryos were used as negative controls.

Luciferase reporter assay

100 pg β-catenin mRNA was co-injected with either 50 pg Super 8X TOPflash (Addgene, #12456) or 50 pg Super 8X FOPflash (Addgene, #12457) into the animal pole region of *Xenopus* embryos at the 1-cell stage, and embryos were incubated at 20 °C until stage 11−12 (middle gastrula). Embryos (three biological replicates) were collected and washed in 0.1x Steinberg solution and homogenized in the luciferase assay system (Promega, E1500) following the manufacturer's guidelines. Lysates were then transferred to individual wells in a 96-well plate, and luciferase activity was measured using a Centro LB960 microplate reader (Berthold Technologies). Statistical analysis was carried out with GraphPad Prism 9 software (www.graphpad.com), and two-way ANOVA was used to analyze statistical significance ($P < 0.05$).

Microinjection for IP-MS analysis

β-catenin mRNA was injected into fertilized *X. laevis* embryos at the 1-cell stage. Due to differences in translation efficiency, the amount of mRNA injected for each metazoan FLAG-tagged β-catenin (3 ng of *B. mikado*

versus 1 ng of *X. laevis*, *E. fluviatilis*, and *N. vectensis*) was optimized such that FLAG-tagged protein expression was roughly equivalent. Uninjected embryos were used as controls. Embryos were then cultured in 1× Steinberg Solution containing 5% Ficoll at 20 °C until stage 12.

Immunoprecipitation and Western blot analysis

Homogenization and immunoprecipitation were as described [79] with slight modifications. Gastrula embryos (18 h post-fertilization (hpf)) were lysed by pipetting in 1 ml ice-cold lysis buffer (20 mM Tris-HCl, pH 8, 70 mM KCl, 1 mM EDTA, 1% NP-40, 10% glycerol and 1× Roche complete proteinase inhibitor cocktail. This was followed by sonication in a water bath at 4 °C for 60 s. The lysate was then clarified by centrifugation for 15 min at 14000 rpm at 4 °C to remove cell debris, pigment, and yolk. Supernatant was recovered, and subsequently, protein concentration was measured using a Direct Detect infrared spectrometer (Merck). Aliquots of supernatant were then snap-frozen in liquid nitrogen and stored at -80 °C. For immunoprecipitation, lysate containing 3 mg total protein was mixed with 40 μl anti-FLAG M2 magnetic beads (Sigma Aldrich) in 1000 μl, and incubated overnight at 4 °C. Beads were then washed three times with 500 μl cold lysis buffer and resuspended in 65 μl 2× sample buffer (Nacalai). For western blot analysis, sample buffer was added to protein lysates or IP elutes and boiled at 95 °C for 5 min. Subsequently, equivalent amounts of protein were separated on SDS-PAGE and transferred to a PVDF membrane (Biorad). The following antibodies were used for protein blotting: TUBA1A (Sigma-Aldrich, T6074, 1/1000), CTNNA1 (Santacruz, sc-9988, 1/500), FLAG-tag sequence (Sigma-Aldrich, F1804, 1/1000), and GAPDH (Santacruz, sc-47724, 1/1000). Signals were developed with horseradish peroxidase-conjugated goat against mouse secondary antibody (Jackson Immuno Research, 115035003, 1/10000) and chemiluminescence was developed by treating the membrane with ImmunoStar Zeta (Wako Pure Chemical Industries).

In-gel trypsin digestion

45 μl of elute were loaded into lanes of a 7.5% polyacrylamide gel for SDS-PAGE. Protein bands were visualized using SimplyBlue SafeStain (Thermo Fisher Scientific). Using a clean scalpel, individual gel lanes were excised into six fractions from high to low molecular weight. These fractions were further diced into small pieces (2 mm^3) and transferred to a low-binding, 96-well Eppendorf plate. Briefly, gel pieces were washed with MilliQ water, followed by 50 mM ammonium bicarbonate in 50% (vol/vol) acetonitrile and shrunken by adding 100% acetonitrile for 5 min. Proteins were reduced at 56°C with 160 μl of 10 mM dithiothreitol in 50 mM ammonium bicarbonate for 30 min and then alkylated with 160 μl

of 55 mM iodoacetamide in 50 mM ammonium bicarbonate for 30 min in darkness. Finally, gel pieces were washed with 50 mM ammonium bicarbonate in 50% (vol/vol) acetonitrile, followed by 100% acetonitrile to complete dryness. Gel pieces were rehydrated with 15 µl of 10 ng/µl trypsin in digestion buffer (50 mM ammonium bicarbonate containing 10% (vol/vol) acetonitrile) for 15 min. The liquid volume was adjusted with 60 µl of digestion buffer to prevent sample drying, and pieces were incubated overnight at 37 ℃. Digestion was stopped by adding formic acid to achieve a final concentration of 5%, and supernatant was transferred into a new 96-well plate. Tryptic peptides were extracted from the gel by adding 100 µl of 50% acetonitrile/ 5% formic acid (vol/vol) for 45 min, followed by 100 µl of 100% acetonitrile for 5 min. Extracted peptides were pooled in the 96-well plate and concentrated by vacuum centrifugation at 42 ℃ for 2 h using the HPLC method of a Genevac EZ-2 Elite (ATS) vacuum evaporator. Dried peptides were desalted using C_{18} StageTips [80]. Briefly, C_{18} StageTips were prepared by packing C_{18} solid phase extraction disks (CDS Empore™) in 200 µl tips, activated with 100 µl of 80% acetonitrile/ 0.1% formic acid (vol/vol) and conditioned with 200 µl of 1% acetic acid/ 0.5% formic acid (vol/vol). Peptides were resuspended in 50 µl of 1% acetic acid/ 0.5% formic acid (vol/vol) and then loaded onto C_{18} StageTips. After washing with 200 µl of 0.1% formic acid, peptides were eluted with 100 µl of 80% acetonitrile/ 0.1% formic acid and dried using the vacuum evaporator as described above.

LC-MS/MS analysis

Dried peptides were resuspended in 25 µl of 5% methanol/ 0.1% formic acid in MilliQ water (vol/vol), and separated with an ultrahigh-performance liquid chromatography system (Waters nanoACQUITY UPLC, Waters) on a trap column (2 cm x 180 µm, nanoEase M/Z Symmetry C_{18} Trap Column, Waters), and a separation column (15 cm x 75 µm, nanoEase M/Z HSS T3 Column, Waters). Solvent A was 0.1% formic acid and solvent B was 0.1% formic acid in 80% acetonitrile. The column temperature was set to 40 ℃. The UPLC system was coupled online to an Orbitrap Fusion Lumos mass spectrometer (Thermo Fisher Scientific). For each sample, 5 µl were injected, and peptides were separated at a flow rate of 0.5 µl/min using a one-hour gradient of 1–50% solvent B. The mass spectrometer was set to perform data acquisition in positive-ion mode at a resolution of 120 K, MS1 scan range between 400 and 1500 m/z, a maximum ion accumulation time of 50 msec with an AGC target of 4.0e5. Other settings included 3 s between master scans (MS1), activation of monoisotopic peak determination of peptide (MIPS), and an ion isolation window of 1.2 m/z. MS2 spectra were analyzed either by the Orbitrap or the linear ion trap using the CHOPIN method [81], depending on the charge and intensity of the peak. Precursor ions carrying 2+charges were fragmented with collision-induced dissociation (CID) in the ion trap at a collision energy of 35%.

Precursor charges from 3+to 7+with precursor intensity greater than 5.0^{e5} were fragmented with High Collision Dissociation (HCD) in the orbitrap at a collision energy of 25% and the orbitrap resolution set at 15 K. The remaining ions, with charges from 3+to 7+with precursor intensity less than 5.0^{e5}, were fragmented with CID as above. Dynamic exclusion was applied after 1 event for 12 s with a mass tolerance of 10 ppm.

Data analysis

All MS and MS/MS spectra were analyzed with Proteome Discoverer software V2.2 (Thermo Fisher Scientific, Inc) with the SEQUEST HT search engine for protein identification and label-free quantitation. Database searches were performed against the Uniprot *X. laevis* database (11/Dec/2019; 57070 entries) and the common Repository of Adventitious Proteins (cRAP; http://www.thegpm.org/crap/). Search parameters for identification were trypsin enzyme, allowing up to two missed cleavages, with precursor and fragment mass tolerance set to 20 ppm and 0.8 Da, respectively. Carboxyamidomethylation of cysteine was set as a fixed modification, while methionine oxidation, asparagine, glutamine deamidation, and N-terminal acetylation were variable modifications. Results were filtered using a False Discovery Rate (FDR) of <1% as a cutoff threshold at the protein level, determined by the Percolator algorithm in Proteome Discoverer software. Protein abundances in each fraction were summed and normalized using the "Total Peptide Amount" setting. For IP samples, protein ratio calculations were performed using pairwise ratios and proteins identified in at least two of three replicates were included in the statistical analysis. Differences in protein composition was evaluated using background-based ANOVA analysis, as implemented in Proteome Discoverer. Proteins were considered significantly changed if the log2 fold change in abundance between the control (uninjected) and sample was greater than 1, with an adjusted p value less than 0.05.

Supplementary Information

Supplementary Material 1

Supplementary Material 2

Supplementary Material 3

Supplementary Material 4

Supplementary Material 5

Supplementary Material 6

Supplementary Material 7

Supplementary Material 8

Supplementary Material 9

Supplementary Material 10

Supplementary Material 11

Supplementary Material 12

Supplementary Material 13

Supplementary Material 14

Supplementary Material 15

Supplementary Material 16

Author contributions
IM, HW conceived and designed this study. IM carried out most experiments and analyzed data. CK, AVB, YH, HE carried out proteomic experiments and data analysis. YT, KT performed 3D modelling. YY instructed IM on experiments using *Xenopus* embryos. IM, CK, KT, HW wrote the manuscript. All authors have read and approved the manuscript.

Data availability
All raw LC-MS/MS data have been deposited at the ProteomeXchange Consortium (http://proteomecentral.proteomexchange.org) via jPOST (https://jpostdb.org*)* [83] with the data set identifier < PXD053223>. Proteome Discoverer output is also available on ProteomeXchange Consortium with the same identifier as above. Other datasets and plasmids used in this study are available from the corresponding author upon request.

Declarations

Ethics approval
All experiments and procedures carried out using *Xenopus laevis* were approved by the Okinawa Institute of Science and Technology Graduate University's Animal Care and Use Committee (Approval ID: 2020-308-2).

Consent for publication
Not applicable.

Competing interests
The authors have no conflicts of interest.

Received: 26 June 2024 / Accepted: 22 October 2024
Published online: 02 December 2024

References
1. Clarke DN, Miller PW, Lowe CJ, Weis WI, Nelson WJ. Characterization of the cadherin-catenin complex of the Sea Anemone Nematostella vectensis and implications for the evolution of Metazoan Cell-Cell Adhesion. Mol Biol Evol. 2016;33:2016–29.
2. Nathaniel Clarke D, Lowe CJ, James Nelson W. The cadherin-catenin complex is necessary for cell adhesion and embryogenesis in Nematostella vectensis. Dev Biol. 2019;447:170–81.
3. Schippers KJ, Nichols SA. Evidence of signaling and adhesion roles for β-Catenin in the Sponge Ephydatia muelleri. Mol Biol Evol. 2018;35:1407–21.
4. Pang K, Ryan JF, Mullikin JC, Baxevanis AD, Martindale MQ. Genomic insights into wnt signaling in an early diverging metazoan, the ctenophore Mnemiopsis leidyi. Evodevo. 2010;1:1–15.
5. MacDonald BT, Tamai K, He X. Wnt/β-Catenin signaling: components, mechanisms, and diseases. Dev Cell. 2009;17:9–26.
6. Rigo-Watermeier T, Kraft B, Ritthaler M, Wallkamm V, Holstein T, Wedlich D. Functional conservation of Nematostella Wnts in canonical and noncanonical wnt-signaling. Biol Open. 2012;1:43.
7. Kraus Y, Aman A, Technau U, Genikhovich G. Pre-bilaterian origin of the blastoporal axial organizer. Nat Commun. 2016;7:1–9.
8. Momose T, Houliston E. Two oppositely localised frizzled RNAs as axis determinants in a cnidarian embryo. PLoS Biol. 2007;5:889–99.
9. Lapébie P, Ruggiero A, Barreau C, Chevalier S, Chang P, Dru P, et al. Differential responses to wnt and PCP disruption predict expression and developmental function of conserved and novel genes in a cnidarian. PLoS Genet. 2014;10:e1004590.
10. Lebedeva T, Aman AJ, Graf T, Niedermoser I, Zimmermann B, Kraus Y, et al. Cnidarian-bilaterian comparison reveals the ancestral regulatory logic of the β-catenin dependent axial patterning. Nat Commun. 2021;12:4032.
11. Röttinger E, Dahlin P, Martindale MQ. A framework for the establishment of a cnidarian gene regulatory network for endomesoderm specification: the inputs of ß-catenin/TCF signaling. PLoS Genet. 2012;8:e1003164.
12. Kraus Y, Fritzenwanker JH, Genikhovich G, Technau U. The blastoporal organiser of a sea anemone. Curr Biol. 2007;17:R874–6.
13. Broun M, Gee L, Reinhardt B, Bode HR. Formation of the head organizer in hydra involves the canonical wnt pathway. Development. 2005;132:2907–16.
14. MacWilliams HK. Hydra transplantation phenomena and the mechanism of Hydra head regeneration. II. Properties of the head activation. Dev Biol. 1983;96:239–57.
15. Reddy PC, Gungi A, Pradhan US, SJ K. Molecular signature of an ancient organizer regulated by Wnt/β-catenin signalling during primary body axis patterning in Hydra. Commun Biol. 2019;2:434.
16. Leininger S, Adamski M, Bergum B, Guder C, Liu J, Laplante M, et al. Developmental gene expression provides clues to relationships between sponge and eumetazoan body plans. Nat Commun. 2014;5:1–15.
17. Adamska M, Degnan SM, Green KM, Adamski M, Craigie A, Larroux C, et al. Wnt and TGF-β expression in the sponge Amphimedon Queenslandica and the origin of metazoan embryonic patterning. PLoS ONE. 2007;2:e1031.
18. Jager M, Dayraud C, Mialot A, Quéinnec E, Le Guyader H, Manuel M. Evidence for involvement of wnt signalling in body polarities, cell proliferation, and the neuro-sensory system in an adult ctenophore. PLoS ONE. 2013;8.
19. Tian Q, Feetham MC, Tao WA, He XC, Li L, Aebersold R, et al. Proteomic analysis identifies that 14-3-3 interacts with beta-catenin and facilitates its activation by Akt. Proc Natl Acad Sci U S A. 2004;101:15370–5.
20. Semaan C, Henderson BR, Molloy MP. Proteomic screen with the proto-oncogene beta-catenin identifies interaction with golgi coatomer complex I. Biochem Biophys Rep. 2019;19:100662.
21. Amit C, Padmanabhan P, Narayanan J. Deciphering the mechanoresponsive role of β-catenin in keratoconus epithelium. Sci Rep. 2020;10:1–16.
22. Hwang JR, Chou CL, Medvar B, Knepper MA, Jung HJ. Identification of β-catenin-interacting proteins in nuclear fractions of native rat collecting duct cells. Am J Physiol Ren Physiol. 2017;313:F30–46.
23. Royo JL, Maeso I, Irimia M, Gao F, Peter IS, Lopes CS, et al. Transphyletic conservation of developmental regulatory state in animal evolution. Proc Natl Acad Sci U S A. 2011;108:14186–91.
24. Vogg MC, Beccari L, Iglesias Ollé L, Rampon C, Vriz S, Perruchoud C, et al. An evolutionarily-conserved Wnt3/β-catenin/Sp5 feedback loop restricts head organizer activity in Hydra. Nat Commun. 2019;10:1–15.
25. Richards GS, Simionato E, Perron M, Adamska M, Vervoort M, Degnan BM. Sponge genes provide New Insight into the Evolutionary Origin of the Neurogenic Circuit. Curr Biol. 2008;18:1156–61.

26. Hobmayer B, Rentzsch F, Kuhn K, Happel CM, von Laue CC, Snyder P, et al. WNT signalling molecules act in axis formation in the diploblastic metazoan Hydra. Nature. 2000;407:186–9.

27. Ziegler B, Yiallouros I, Trageser B, Kumar S, Mercker M, Kling S, et al. The wnt-specific astacin proteinase HAS-7 restricts head organizer formation in Hydra. BMC Biol. 2021;19:1–22.

28. Yasuoka Y, Kobayashi M, Kurokawa D, Akasaka K, Saiga H, Taira M. Evolutionary origins of blastoporal expression and organizer activity of the vertebrate gastrula organizer gene lhx1 and its ancient metazoan paralog lhx3. Development. 2009;136:2005–14.

29. Gul IS, Hulpiau P, Saeys Y, Roy F. Metazoan evolution of the armadillo repeat superfamily. Cell Mol Life Sci. 2017;74:525–41.

30. Graham TA, Weaver C, Mao F, Kimelman D, Xu W. Crystal structure of a β-Catenin/Tcf complex. Cell. 2000;103:885–96.

31. Belahbib H, Renard E, Santini S, Jourda C, Claverie JM, Borchiellini C, et al. New genomic data and analyses challenge the traditional vision of animal epithelium evolution. BMC Genomics. 2018;19:1–15.

32. Von Kries JP, Winbeck G, Asbrand C, Schwarz-Romond T, Sochnikova N, Dell'Oro A, et al. Hot spots in β-catenin for interactions with LEF-1, conduction and APC. Nat Struct Biol. 2000;7:800–7.

33. Fasolini M, Wu X, Flocco M, Trosset JY, Oppermann U, Knapp S. Hot spots in Tcf4 for the interaction with β-catenin. J Biol Chem. 2003;278:21092–8.

34. Vleminckx K, Kemler R, Hecht A. The C-terminal transactivation domain of β-catenin is necessary and sufficient for signaling by the LEF-1/β-catenin complex in Xenopus laevis. Mech Dev. 1999;81:65–74.

35. Su H, Sureda-Gomez M, Rabaneda-Lombarte N, Gelabert M, Xie J, Wu W. A C-terminally truncated form of β-catenin acts as a novel regulator of Wnt/β-catenin signaling in planarians. PLoS Genet. 2017;13:e1007030.

36. Schneider SQ, Finnerty JR, Martindale MQ. Protein evolution: structure-function relationships of the oncogene beta-catenin in the evolution of multicellular animals. J Exp Zool. 2003;295B:25–44.

37. DuChez BJ, Hueschen CL, Zimmerman SP, Baumer Y, Wincovitch S, Playford MP. Characterization of the interaction between β-catenin and sorting nexin 27: contribution of the type I PDZ-binding motif to wnt signaling. Biosci Rep. 2019;39:BSR20191692.

38. Gallet A, Angelats C, Erkner A, Charroux B, Fasano L, Kerridge S. The C-terminal domain of Armadillo binds to hypophosphorylated Teashirt to modulate wingless signalling in Drosophila. EMBO J. 1999;18:2208–17.

39. Aberle H, Schwartz H, Hoschuetzky H, Kemler R. Single amino acid substitutions in proteins of the armadillo gene family abolish their binding to α-catenin. J Biol Chem. 1996;271:1520–6.

40. Piedra J, Miravet S, Castaño J, Pálmer HG, Heisterkamp N, García de Herreros A, et al. p120 catenin-Associated Fer and Fyn Tyrosine Kinases regulate β-Catenin Tyr-142 phosphorylation and β-Catenin-α-Catenin Interaction. Mol Cell Biol. 2003;23:2287–97.

41. Wikramanayake AH, Hong M, Lee PN, Pang K, Byrum CA, Bince JM, et al. An ancient role for nuclear β-catenin in the evolution of axial polarity and germ layer segregation. Nature. 2003;426:446–50.

42. Lebedeva T, Boström J, Mörsdorf D, Niedermoser I, Genikhovich E, Adameyko I, et al. β-catenin-dependent endomesoderm specification appears to be a Bilateria-specific co-option. Biorxiv. 2022. https://doi.org/10.1101/2022.10.15.512282.

43. Lapébie P, Gazave E, Ereskovsky A, Derelle R, Bézac C, Renard E, et al. WNT/β-Catenin signalling and epithelial patterning in the Homoscleromorph Sponge Oscarella. PLoS ONE. 2009;4:e5823.

44. Molenaar M, van de Wetering M, Oosterwegel M, Peterson-Maduro J, Godsave S, Korinek V, et al. XTcf-3 transcription factor mediates β-Catenin-Induced Axis formation in Xenopus embryos. Cell. 1996;86:391–9.

45. Griffin JN, del Viso F, Duncan AR, Robson A, Hwang W, Kulkarni S, et al. RAPGEF5 regulates Nuclear translocation of β-Catenin. Dev Cell. 2018;44:248–e2604.

46. Xu Z, He W, Ke T, Zhang Y, Zhang G. DHRS12 inhibits the proliferation and metastasis of osteosarcoma via Wnt3a/β-catenin pathway. Future Oncol. 2020;16:665–74.

47. Hachimi M, Grabowski C, Campanario S, Herranz G, Baonza G, Serrador JM, et al. Smoothelin-like 2 inhibits Coronin-1B to stabilize the apical actin cortex during Epithelial Morphogenesis. Curr Biol. 2021;31:696–e7069.

48. Sroka R, van Lint J, Katz SF, Schneider MR, Kleger A, Paschke S, et al. Cortactin is a scaffolding platform for the E-cadherin adhesion complex and is regulated by protein kinase D1 phosphorylation. J Cell Sci. 2016;129:2416–29.

49. Alié A, Hayashi T, Sugimura I, Manuel M, Sugano W, Mano A, et al. The ancestral gene repertoire of animal stem cells. Proc Natl Acad Sci U S A. 2015;112:E7093–100.

50. Ehyai S, Miyake T, Williams D, Vinayak J, Bayfield MA, McDermott JC. FMRP recruitment of β-catenin to the translation pre-initiation complex represses translation. EMBO Rep. 2018;19:e45536.

51. an de Wetering M, Cavallo R, Dooijes D, van Beest M, van Es J, Loureiro J, et al. Armadillo coactivates transcription driven by the product of the Drosophila segment polarity gene dTCF. Cell. 1997;88:789–99.

52. Hsu S-C, Galceran J, Grosschedl R. Modulation of Transcriptional Regulation by LEF-1 in response to Wnt-1 signaling and Association with β-Catenin. Mol Cell Biol. 1998;18:4807–18.

53. Xing Y, Takemaru KI, Liu J, Berndt JD, Zheng JJ, Moon RT, et al. Crystal structure of a full-length β-Catenin. Structure. 2008;16:478–87.

54. Lam AK, Phillips BT. Wnt signaling polarizes asymmetric cell divisions during development. Results Probl Cell Differ. 2017;61:83–114.

55. Schneider SQ, Bowerman B. β-Catenin asymmetries after all Animal/Vegetal- oriented cell divisions in Platynereis dumerilii embryos mediate binary cell-fate specification. Dev Cell. 2007;13:73–86.

56. Phillips BT, Kidd AR, King R, Hardin J, Kimble J. Reciprocal asymmetry of SYS-1/β-catenin and POP-1/TCF controls asymmetric divisions in Caenorhabditis elegans. Proc Natl Acad Sci U S A. 2007;104:3231–6.

57. Huang S, Shetty P, Robertson SM, Lin R. Binary cell fate specification during C. Elegans embryogenesis driven by reiterated reciprocal asymmetry of TCF POP-1 and its coactivator beta-catenin SYS-1. Development. 2007;134:2685–95.

58. Lawo S, Bashkurov M, Mullin M, Ferreria MG, Kittler R, Habermann B, et al. HAUS, the 8-Subunit Human Augmin Complex, regulates Centrosome and Spindle Integrity. Curr Biol. 2009;19:816–26.

59. Wu G, Lin Y-T, Wei R, Chen Y, Shan Z, Lee W-H. Hice1, a Novel Microtubule-Associated Protein Required for Maintenance of Spindle Integrity and Chromosomal Stability in Human cells. Mol Cell Biol. 2008;28:3652.

60. Mbom BC, Nelson WJ, Barth A. β-catenin at the centrosome. BioEssays. 2013;35:804–9.

61. Spink KE, Fridman SG, Weis WI. Molecular mechanisms of β-catenin recognition by adenomatous polyposis coli revealed by the structure of an APC–β-catenin complex. EMBO J. 2001;20:6203.

62. Mizumoto K, Sawa H. Cortical β-Catenin and APC regulate Asymmetric Nuclear β-Catenin localization during asymmetric cell division in C. Elegans. Dev Cell. 2007;12:287–99.

63. Louie RK, Bahmanyar S, Siemers KA, Votin V, Chang P, Stearns T, et al. Adenomatous polyposis coli and EB1 localize in close proximity of the mother centriole and EB1 is a functional component of centrosomes. J Cell Sci. 2004;117:1117–28.

64. Dikovskaya D, Newton IP, Näthke IS. The adenomatous polyposis coli protein is required for the formation of robust spindles formed in CSF Xenopus extracts. Mol Biol Cell. 2004;15:2978–91.

65. Lui C, Ashton C, Sharma M, Brocardo MG, Henderson BR. APC functions at the centrosome to stimulate microtubule growth. Int J Biochem Cell Biol. 2016;70:39–47.

66. Raemaekers T, Ribbeck K, Beaudouin J, Annaert W, van Camp M, Stockmans I, et al. NuSAP, a novel microtubule-associated protein involved in mitotic spindle organization. J Cell Biol. 2003;162:1017–29.

67. Yamada K, Tomii K. Revisiting amino acid substitution matrices for identifying distantly related proteins. Bioinformatics. 2014;30:317–25.

68. Zimmermann L, Stephens A, Nam SZ, Rau D, Kübler J, Lozajic M, et al. A completely reimplemented MPI Bioinformatics Toolkit with a new HHpred server at its core. J Mol Biol. 2018;430:2237–43.

69. Deorowicz S, Debudaj-Grabysz A, Gudys A. FAMSA: fast and accurate multiple sequence alignment of huge protein families. Sci Rep. 2016;6:1–13.

70. Webb B, Sali A. Comparative protein structure modeling using MODELLER. Curr Protoc Bioinf. 2016;2016:5.6.1–5.6.37.

71. Tomii K, Hirokawa T, Motono C. Protein structure prediction using a variety of profile libraries and 3D verification. Proteins: Structure, Function, and Bioinformatics. 2005;61:114–21.

72. Laskowski RA, MacArthur MW, Moss DS, Thornton JM. PROCHECK: a program to check the stereochemical quality of protein structures. J Appl Crystallogr. 1993;26:283–91.

73. Ramachandran GN, Ramakrishnan C, Sasisekharan V. Stereochemistry of polypeptide chain configurations. J Mol Biol. 1963;7:95–9.

74. Pettersen EF, Goddard TD, Huang CC, Couch GS, Greenblatt DM, Meng EC, et al. UCSF Chimera - A visualization system for exploratory research and analysis. J Comput Chem. 2004;25:1605–12.

75. Edgar RC. MUSCLE: multiple sequence alignment with high accuracy and high throughput. Nucleic Acids Res. 2004;32:1792–7.

76. Bailey TL, Boden M, Buske FA, Frith M, Grant CE, Clementi L et al. MEME SUITE: tools for motif discovery and searching. Nucleic Acids Res. 2009;37 Web Server issue:W202-8.

77. Wlizla M, McNamara S, Horb ME. Generation and care of Xenopus laevis and Xenopus tropicalis embryos. Methods Mol Biol. 2018;1865:19.

78. Nieuwkoop P, Faber J, Gerhart J, Kirschner M. Normal Table of Xenopus Laevis (Daudin) : A Systematical and Chronological Survey of the Development from the Fertilized Egg Till the End of Metamorphosis. Normal Table of Xenopus Laevis (Daudin). 2020. https://doi.org/10.1201/9781003064565

79. Akkers RC, Jacobi UG, Veenstra GJC. Chromatin immunoprecipitation analysis of Xenopus embryos. Methods Mol Biol. 2012;917:279–92.

80. Rappsilber J, Mann M, Ishihama Y. Protocol for micro-purification, enrichment, pre-fractionation and storage of peptides for proteomics using StageTips. Nat Protoc. 2007;2:1896–906.

81. Davis S, Charles PD, He L, Mowlds P, Kessler BM, Fischer R. Expanding Proteome Coverage with CHarge ordered parallel Ion aNalysis (CHOPIN) combined with broad specificity proteolysis. J Proteome Res. 2017;16:1288–99.

Publisher's note

Springer Nature remains neutral with regard to jurisdictional claims in published maps and institutional affiliations.